B-SPLINE PRCESSING OF 90W-7Ni-3Fe WHA DILATOMETRIC DATA

Andrzej J. Panas

Military University of Technology, Kaliskiego 2 Street, 00-908 Warsaw, Poland

Andrzej.Panas@wat.edu.pl

Abstract:

B-spline approximation procedure applied to fitting the high thermal resolution thermophysical data is presented. The procedure has been used for characterisation of a 2-nd order phase transition revealed in dilatometric measurements of 90W-7Ni-3Fe tungsten heavy alloy (WHA). The experiments have been performed applying laser interferometry apparatus. Both the coefficient of linear thermal expansion (CLTE) and the linear expansivity (LE) data from thermal cycling within 20 ^{o}C and 1120 ^{o}C have been processed. As a result representative characteristics have been obtained. The discussed algorithm has been proved to be efficient in scattered thermophysical data processing.

1. Introduction

Almost every process of thermophysical property characterisation involves the experimental data processing. Usually data are processed for the purpose of introducing the appropriate characteristic into the appropriate database or for its thorough examination. In the first case the problem typically reduces to data averaging. In the second, needs of precise material diagnostics force more thorough examination of the experimental results. A special care is needed when the high thermal resolution data are handled. High thermal resolution means that a certain property is obtained within a very small temperature interval. Such data usually need to be approximated. The problem with approximation is proper selection of the functional basis. In typical cases theoretical indications for a certain functional dependence on the temperature are very weak [1]. In such situation polynomials are usually utilised. However, it was proved that due to many disadvantages single polynomials should be excluded from fitting high resolution thermophysical data [2]. Polynomials are not only badly numerically conditioned [3] but also proved to be inefficient in reconstruction of discontinuities of the investigated functional dependence [4]. On the other hand there is a broad range of possibilities connected with utilisation of splines [5]. Strangely enough, spline functions have rarely been used for that purpose despite the fact that even in a fundamental work of de Boor, titanium specific heat data were applied as an illustrative example of their application [4]. Splines, in that range basis splines (B-splines), exhibit unique features that predestine them to be used for approximation of high resolution thermophysical data. The most important is the possibility of almost unrestricted global and local reconstruction of not only the function but its derivatives as well. This particular feature can be effectively exploited for characterisation of materials exhibiting phase transition [7].

In this work s spline approximation of the high thermal resolution diltometric data (comp. [8]) from investigations of a 90W-7Ni-3Fe tungsten heavy alloy (WHA) is discussed. Tungsten heavy alloys are high–density dispersed composite materials in which quasi-spherical hard tungsten particles are embedded in a ductile matrix [8, 9]. Due to specific combination of mechanical properties, namely high strength and hardness together with good ductility, these alloys have been found increasingly applicable in nuclear and military technologies. The discussed studies of the thermal expansivity are comprised within the frame of a wider research programme on WHSs and related materials. The main purpose of the investigation is

characterisation of all thermophysical properties to complement the literature in that domain (comp. eg. [9]). The data will also be exploited in numerical modelling of selected processes of WHA sintering technology.

2. B-spline Approximation

The details concerning the theory of spline functions can be found elsewhere (comp. e.g. [4] and [5]). For the purpose of this work let us just summarise basic facts about splines. A spline function can be defined within a closed interval containing the data [T_a, T_b], where T is the temperature. Let $\{\tau_i\}_1^n$, $T_a \le \tau_i \le T_b$ be a nondecreasing sequence of n points called knots. Let $\{\xi_k\}_1^N$ be a strictly increasing sequence composed of the previous one in such a way that all repetitions of τ_i are excluded. The points ξ_k are called breakpoints. In relation to these two sequences we define another sequence $\{\nu_k\}_1^N$ which counts repetitions of ξ_k in $\{\tau_i\}_1^n$ defining multiplicity of knots.

A spline of order r on [T_a, T_b] with reference to a multiple knot sequence $\{\tau_i\}_1^n$, $\tau_i < \tau_{i+r}$ is the function $S_r^{\boldsymbol{\tau}}$ which [6]:

a) is a polynomial of order r (degree r-1) within every subinterval $[\xi_k, \xi_{k+1}]$;

b) is a $C^{r-\nu_k-1}$ class function at ξ_k.

In single knot subdivision case the spline is a C^{r-2} class function within the whole interval [a, b] and a C^{r-1} class function within $[a,b]\setminus\{\xi_k\}_1^N$. Multiplication of knots corresponds to lower continuity conditions at breakpoints – if a certain knot is multiplied, then the range of continuity in a corresponding breakpoint is proportionally decreased. For simplicity reasons a knot indication in the notation of splines will be omitted throughout the article.

The spline function S_r can be represented by piecewise polynomial (so called pp-function) of corresponding order r. This representation is equivalent to decomposition of a spline with reference to a base of truncated mononomials [4], [5]:

$$\forall T \in [\xi_k, \xi_{k+1}), k = 1,\ldots,N-1 \quad S_r(T) = \sum_{m=0}^{r-1} c_{km}(T-\xi_k)^m \tag{1}$$

To make this formula complete we take $S(\xi_N) = \lim_{T \to \xi_N} S(T)$. Hence, we conclude that pp-representation for a certain spline consists of: the integers r and N-1 giving order and number of its polynomial pieces, the strictly increasing sequence $\{\xi_k\}_1^N$ of its breakpoints and a matrix $[c_{km}]$ of dimension $(N\text{-}1)\times r$ which is the matrix of its right derivatives at the breakpoints [5]. The mononomials for piecewise polynomial representation of a spline function is shown at Figure 1.

A spline function can also be referred to another functional basis. This basis consists of special splines every one of which is defined on a closed support. These splines are called basis splines or B-splines. We can introduce B-splines of order r on a knot sequnce $\{\tau_i\}_1^n$ using a recurrence relation:

$$B_{i,1}(T) = \begin{cases} 1 & \tau_i \le x < \tau_{i+1} \\ 0 & \text{otherwise} \end{cases} \qquad B_{i,r}(t) = \frac{T-\tau_i}{\tau_{i+r-1}-\tau_i} B_{i,r-1}(T) + \frac{\tau_{i+r}-T}{\tau_{i+r}-\tau_{i+1}} B_{i+1,r-1}(T) \tag{2}$$

For a strictly increasing knot sequence 1-st order B-spline is a constant, 2-nd order is composed of two pieces of a linear function, 3-rd order of three pieces of a square function, etc.

The formula (2) can also be applied for calculation of B-splines defined on multiple knot sequences. Multiplied knots are utilized whenever discontinuities of any range should be modeled.

B-splines of order r create a basis within an interval $[\tau_{r-1}, \tau_{n+1}]$ for any spline S_r in such a way that:

$$S_r(T)=\sum_{i=1}^{l}\alpha_i B_{i,r}(T) \tag{3}$$

B-representation for S_r consists of [4]: the integers r and l, giving the order r and the number of linear parameters, the vector $\boldsymbol{\tau}=\{\tau_i\}_1^n=\{\tau_i\}_1^{l+r}$ containing the knots and the vector $\boldsymbol{\alpha}=\{\alpha_i\}_1^l$ of the coefficients of the spline S_r with respect to the B-spline basis $\{B_{i,r}\}_1^l$. An example of recurrence creation of such a basis is shown in Figure 2. The B-spline basis, contrary to a basis composed of mononomials, is relatively well conditioned which makes numerical calculations more reliable.

The least square approximation of given data $\{(T_i,y_i)\}_1^M$ resolves itself to search the minimum of

$$\Phi(\boldsymbol{\alpha},\boldsymbol{\tau})=\sum_{j=1}^{M}w_i\left[y_j-\sum_{i=1}^{l}\alpha_i B_{i,r,\tau}(T_j)\right]^2 \tag{4}$$

with reference to $\boldsymbol{\tau}$ and $\boldsymbol{\alpha}$ as it was described in [5]. The numbers w_i are weights. For a fixed knot sequence $\boldsymbol{\tau}$, the minimisation simplifies to a linear least squares problem. The situation is different when variations of knots are admissible and one is trying to find the best placement of knots that will minimise the least squares error. In this case the problem (the variable knots problem) doesn't usually result in one optimum unequivocal solution.

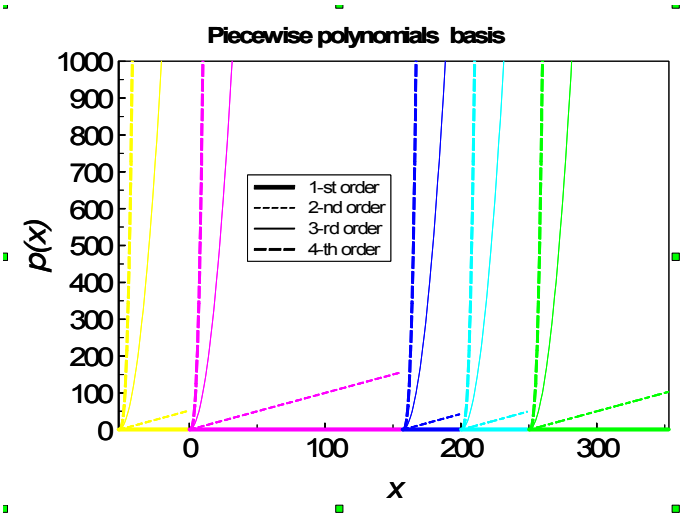

Figure 1. Basis for piecewise polynomial representation of a certain spline within the interval [52; 354] with knots at: -52, 0, 157, 200, 250 and 354

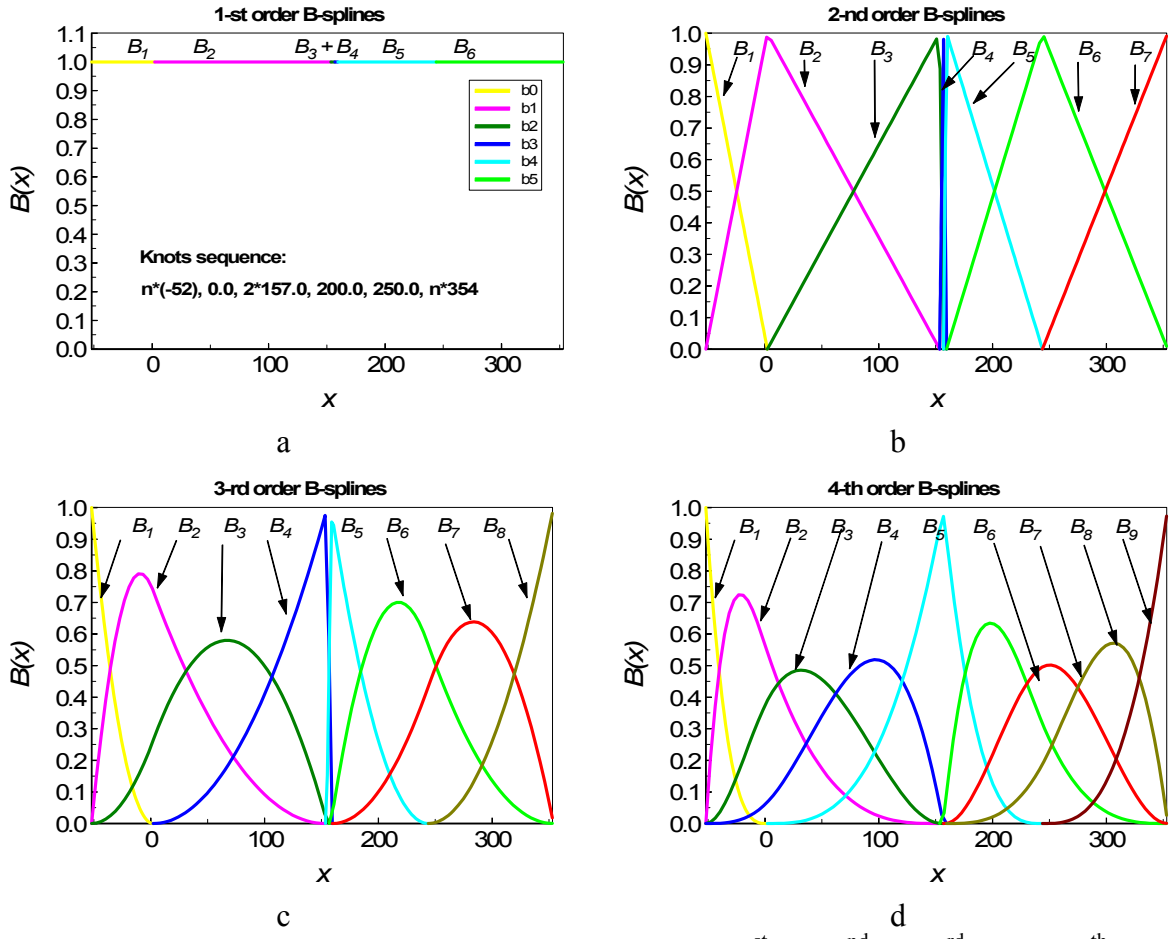

Figure 2. Recurrence construction of a B-spline basis: a - 1st, b – 2nd, c – 3rd and d – 4th order B-splines for the same knot sequence as illustrated in Fig.1

When comparing piecewise polynomial and B-spline representation in solving the approximation problems one can realize that there are strong theoretical and practical indications for preferring the last one. B-splines are better numerically conditioned and easier in recurrence calculations. This makes iterative calculations easier. The B-spline basis is usually composed of not so many functions as in the case of pp-functions. Last but not least it should be underlined that there are both theoretical and practical possibilities of converting splines from B-spline to piecewise polynomial representation.

Determination of the best approximation for a certain experimental data set with utilisation of B-splines resolves itself to the following step by step procedure:

1. Selection of the optimal range *r* of splines to be applied.
2. Determination of a subdivision of the interval $[T_a, T_b]$ comprising the data with simultaneous analysis (identification) of discontinuity points. This step results in definition of the knot sequence (initial knot sequence in a variable knot procedure).
3. Determination of the sequence of *M* weights $\{w_i\}_1^M$.
4. Application of fixed or variable knot procedures and evaluation of results.
5. Possible repetition of steps 1-3 with the order *r* changed or the knot sequence modified. Usually, when variable knot procedures are applied, knots are rearranged according to the obtained results. When certain discontinuities are modeled then fixed knot procedure is preferred in final calculations.
6. Conversion from B-spline to piecewise polynomial representation if necessary.

In numerical calculations described in this paper, both fixed and variable knot procedures were applied. To solve a fixed knot problem, procedures established by the author were used. The variable knot approximation results were obtained with the use of IMSL Fortran procedures that are described in detail in [4].

3. Experimental

Laser Interferometry Dilatometer

Dilatometric measurements were performed using an absolute laser-interferometry apparatus with a microcomputer system for data acquisition and processing (Figure 3). A modified spherical interferometer was utilised. Detailed information of the instrument and the methodology of measurements are given in [7]. The apparatus enables high thermal resolution investigations of CLTE α and linear expansion ε (LE) within a temperature range from –150 K to 1400 K (from about -120 °C to about 1140 °C). Specimens of various shapes can be tested. The actual resolution depends on many factors and affects the accuracy of CLTE determination. Both parameters are correlated and should be analyzed together for every individual case. Test measurements performed for a Cu specimen within the range from 300 to 800 had shown that even if the resolution $\Delta T \cong 2$ K was preserved, the uncertainty could be less than 1 % [7]. Usually the resolution ranges from 0.05 K to 2.0 K.

The measured CLTE values are referred to the room temperature specimen length $l_0=l(t_0=20\ ^{o}\mathrm{C})$ giving experimental standard values of $\alpha^*(t)$ (comp. Figure 4.a)

$$\alpha^*(t)=\frac{1}{l(t_0)}\frac{dl(t)}{dt}=\frac{1}{l_0}\frac{dl(t)}{dt} \tag{5}$$

where t stands for the temperature. The LE is referred to l_0 giving the dilatation denoted here as ε. The LE is calculated by integration of the $\alpha^*(T)$ curve (Figure 4.b)

$$\varepsilon(t)=\frac{l(t)-l(t_0)}{l(t_0)} \tag{6}$$

The data processing is completed with "thermal extortion" diagrams, ie diagrams of the temperature change rate as a function of the actual temperature of the specimen (Figure 4.c).

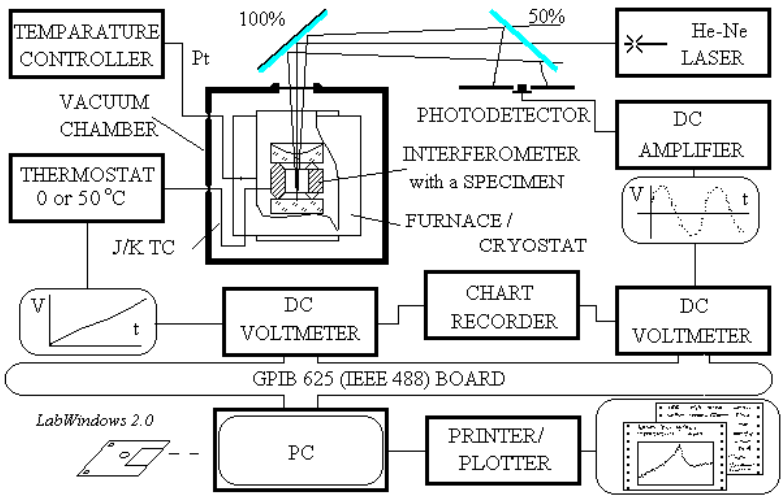

Figure 3. Schematic diagram of the experimental stand

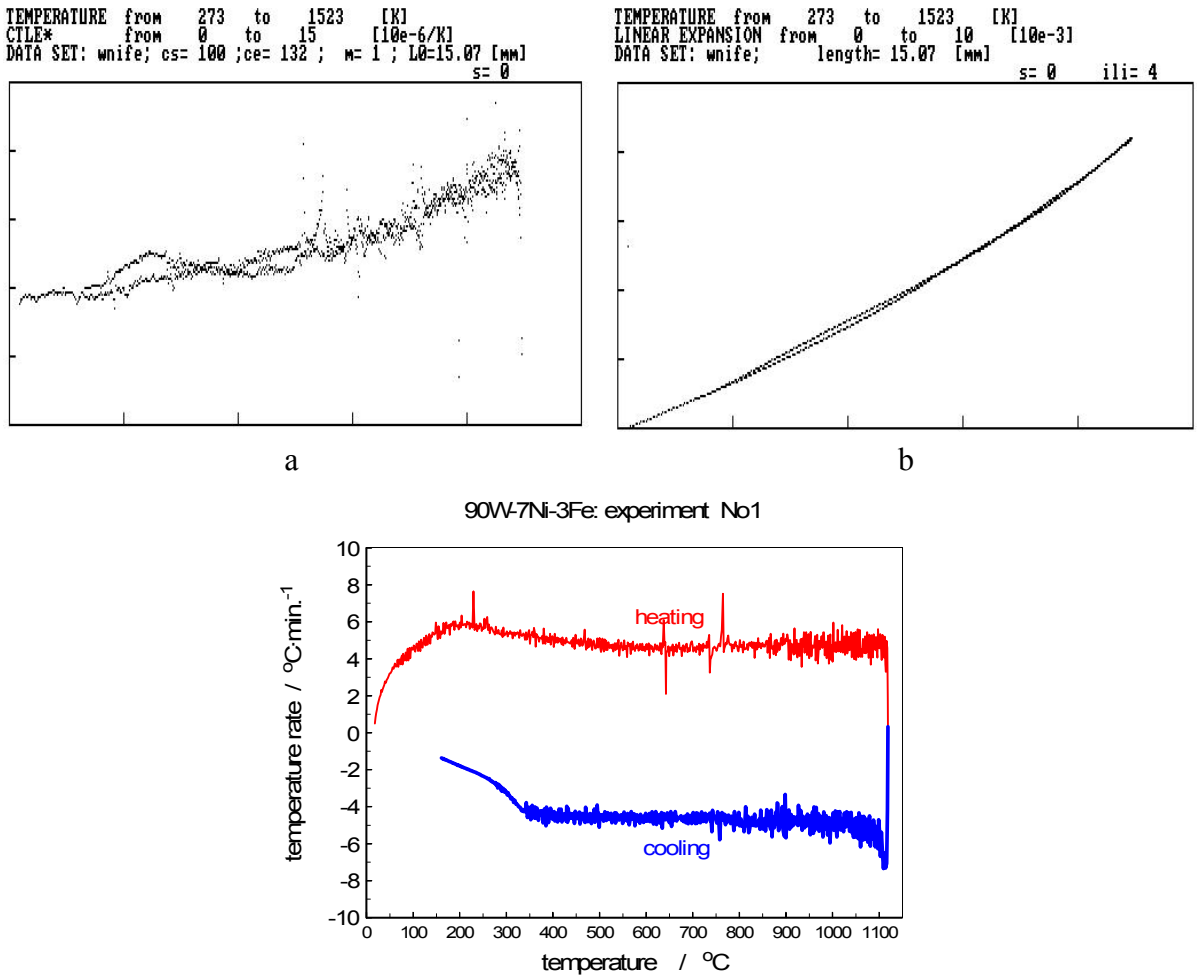

Figure 4. Illustration of typical results from dilatometric investigations: a – measured values of the coefficient of linear thermal expansion (CLTE*) in $10 \cdot K^{-1}$, b – linear expansion (LE) i.e. dilatation in $mm \cdot m^{-1}$ and c – temperature rate versus the specimen temperature (thermal programme). The results shown are obtained at 1-st experimental cycle for the 90W-7Ni-3Fe specimen

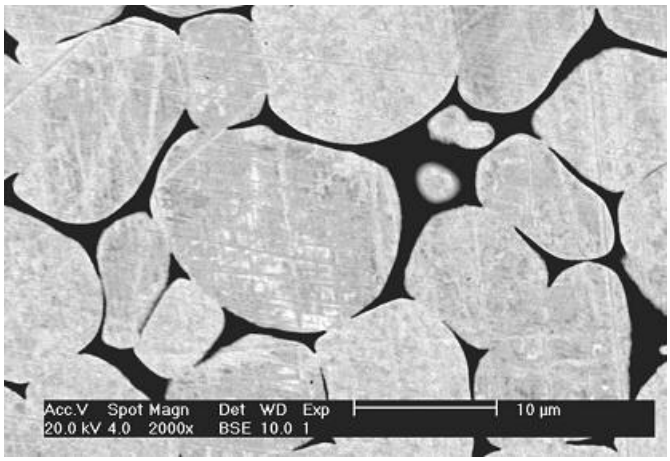

Figure 5. Microstructure of the investigated material: the bright particles are tungsten filler, the dark area is 53Ni-23Fe-24W homogeneous matrix [8]

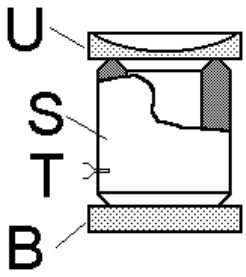

Figure 6. Configuration of the interferometer: U – upper spherical interferometer mirror, B – bottom mirror, T – thermocouple, H – specimen holder, S – cylindrical specimen

Specimen Preparation and Measurement Procedure

The measurements were performed on a 90W-7Ni-3Fe alloy specimen. The numbers in the alloy name stand for the mass composition. The material exhibits typical structure: quasi-spherical hard tungsten particles are embedded in a ductile 53Ni-23Fe-W matrix (Figure 5). The alloy was prepared using standard procedures by sintering its powdered components at about 1650 ^{o}C. Cylindrical specimen was prepared from the finally fabricated ingot by machining to the shape of a hollow cylinder (see Figure 6). The outside diameter of the cylinder was about 19.9 mm, the length was equal to 15.07 mm. The upper horizontal surface of the specimen was cut to ensure a tripod support of the upper interferometer mirror. The dilatometric experiments were carried out under vacuum conditions within the range from room temperature to about 1120 ^{o}C on both heating and cooling over repeated temperature cycles. The heating/cooling rates were usually about 5 K/min. The investigations included four repeated measurements in total.

Results of Experimental Investigations

Dilatometric measurements established experimental thermal characteristics of CLTE* (α*) and dilatation (LE) of the investigated material. The resolution of the recorded data was better than 2 K. The raw experimental data are shown in Figure 4 (1st run) and in Figure 7 (the next three runs).

Inspection of the obtained results revealed phase transition that appeared roughly about 700 ^{o}C. The onset temperature of the transition differ between heating and cooling for about 10÷20 ^{o}C. It was also observed magnification of the CLTE* heating and cooling peaks in every consecutive run. The revealed phase transition results in hysteresises observed on LE curves (Figs 4.b, 7.b, 7.d and 7.f). However, these effects were not accompanied by any permanent changes of the basic specimen length l_0.

4. Numerical Processing of the Experimental Data

Basic tasks of approximation analysis were defined in view of processing of high resolution CLTE* data. They are as follows:

1. Smoothing the dispersed CLTE* data.
2. Reconstruction of the analyzed CLTE* thermal characteristic altogether with its discontinuities due to phase transition.
3. Substitution of discrete data with a representative function enabling data tabulation.

All the above also concerns the dilatation ε. However, there is another task constituting a real challenge:

4. Reconstruction of the CLTE* characteristic using only the LE data.

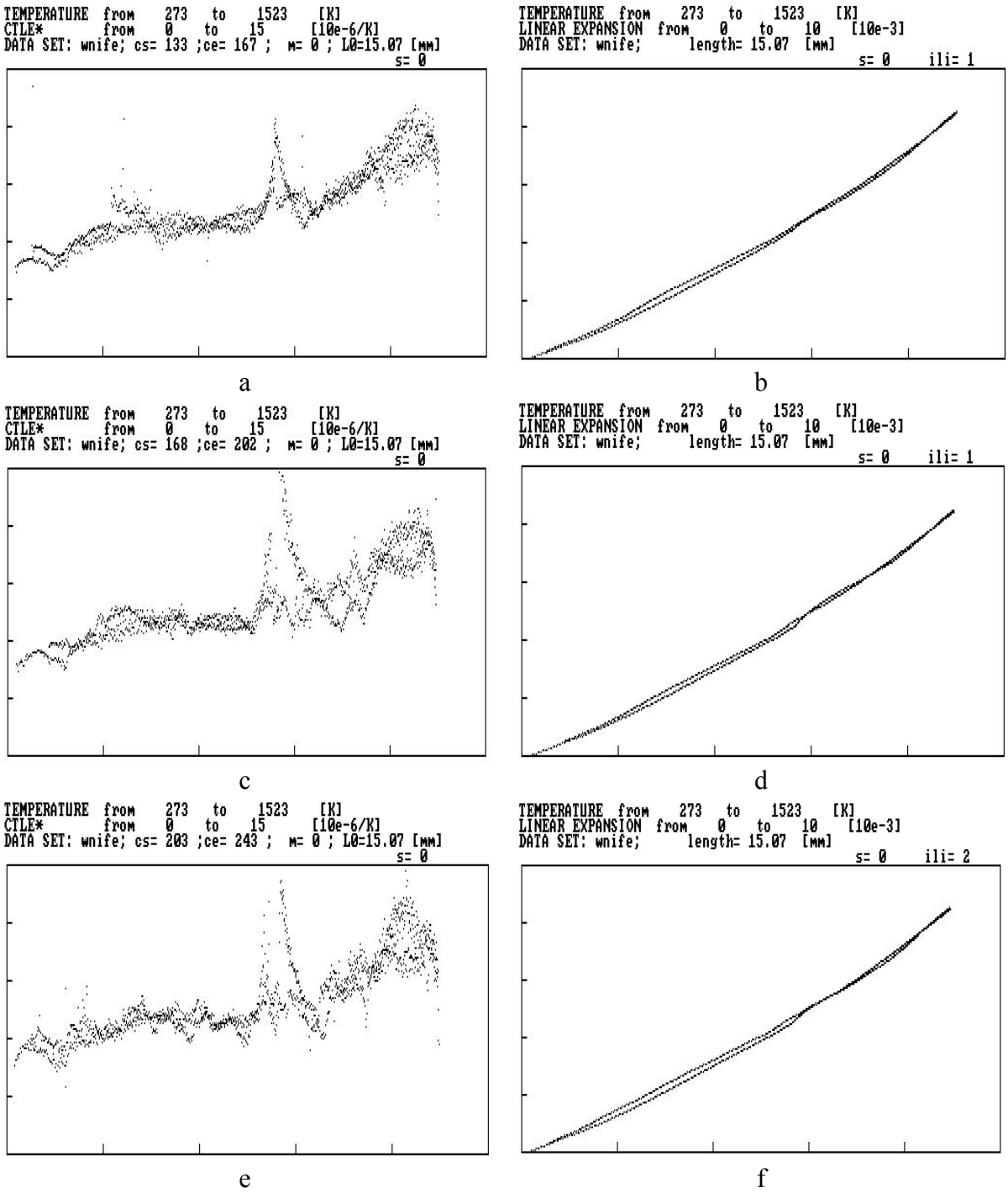

Figure 7. CLTE* and LE results from repeated runs: a, b – 2nd; c, d – 3rd; e, f – 4th

The difficulties in performing the last are mostly due to integral character of dilatation with reference to linear expansivity (comp. eg. [3]).

Basic calculations were performed separately on overlapped heating and overlapped cooling results from all four measurements. Both fixed and variable knot procedures were applied. The uniform weights w_i=1 were taken for the data processing. In calculations 4th order splines were applied. The initial guesses for knots accounted for possible discontinuity of $\alpha^*(T)$ curve at phase transition: corresponding knots at 708 °C for heating and at 695 °C for cooling were multiplied by four. Locations of these crucial knots were established in preliminary calculations – at this stage variable knot procedure was applied once or twice and initial guesses were shifted according to the obtained results. The effects of data processing are shown in Figure 8.

Repeated variable knots calculations applied for compacted CLTE* results made possible more reliable identification of the (averaged) phase transition temperature from sparsely distributed experimental data. Fixed knots algorithm resulted in more reliable representation of the averaged thermal characteristic. Tabulated data and information concerning B-spline representation of the appropriate approximate will not be presented here but it should be mentioned that they are accompanied by a piecewise polynomial representation consisting on 4 and 6 polynomials for heating and cooling respectively (see Tab. 1).

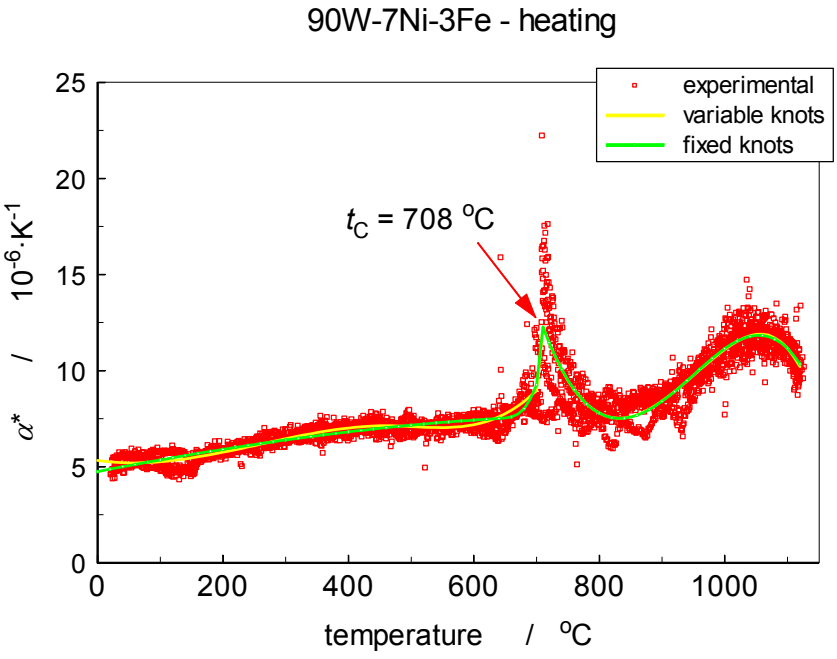

a

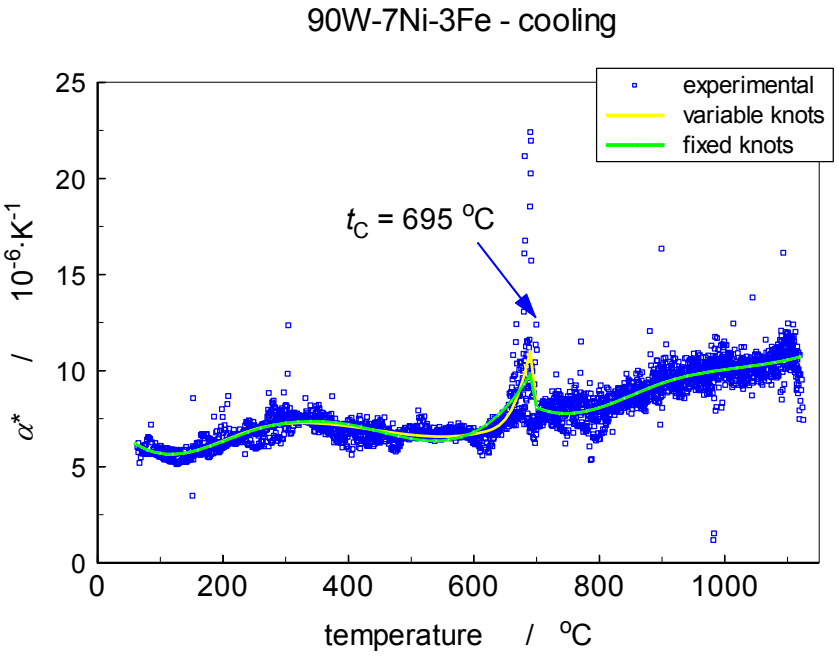

b

Figure 8. Results of B-spline approximation of CLTE* experimental data from: a - heating and b – cooling runs with indication of the identified phase transition peak temperatures

Table 1. Knots distributions for spline characteristics obtained for CLTE* results (data in °C)

Heating (Fig. 8.a)		Cooling (Fig. 8.b)	
Fixed / initial guess	Resultant variable	Fixed / initial guess	Resultant variable
-10	-10	40	40
-10	-10	40	40
-10	-10	40	40
-10	-10	40	40
644	461.9863	250	250
708	706.0758	408	617.3073
708	707.6634	690	689.0349
708	708	695	695
708	708	695	695
940	1003.97	695	695
1140	1140	695	695
1140	1140	905	900.92
1140	1140	1140	1140
1140	1140	1140	1140
		1140	1140
		1140	1140

Table 2. Results of B-spline approximation of LE results from 3rd run

Heating (Fig. 9.a – magenta curve)				Cooling (Fig. 9.a – cyan curve)			
t / °C	LE / mm·m	*t* / °C	LE / mm·m	*t* / °C	LE / mm·m	*t* / °C	LE / mm·m
0	-0.1536	600	3.667983			600	3.787316
50	0.156133	650	4.020009			650	4.137864
100	0.409651	700	4.404421	100	0.481182	700	4.60696
150	0.662437	750	5.021262	150	0.716601	750	4.978506
200	0.938911	800	5.489223	200	1.01746	800	5.356592
250	1.23956	850	5.865678	250	1.357883	850	5.767552
300	1.559742	900	6.223205	300	1.717342	900	6.21928
350	1.895078	950	6.623683	350	2.080658	950	6.701695
400	2.241509	1000	7.113113	400	2.438006	1000	7.198724
450	2.595287	1050	7.688818	450	2.784882	1050	7.703204
500	2.952983	1100	8.278246	500	3.12165	1100	8.218685
550	3.311481	1120	8.48811	550	3.452892	1120	8.430792

For illustration of the algorithm performance in reconstruction of a certain thermal data from its integral characteristic results of linear expansion measurements form the 3rd experiment run were arbitrarily selected. The data were processed applying 5th order splines which correspond to 4th order splines applied in CLTE* approximations. The input data as well as the results of calculations are shown in Figure 9. The illustrated results come from variable knot procedure. The data on LE are additionally presented in tabulated form in Table 2.

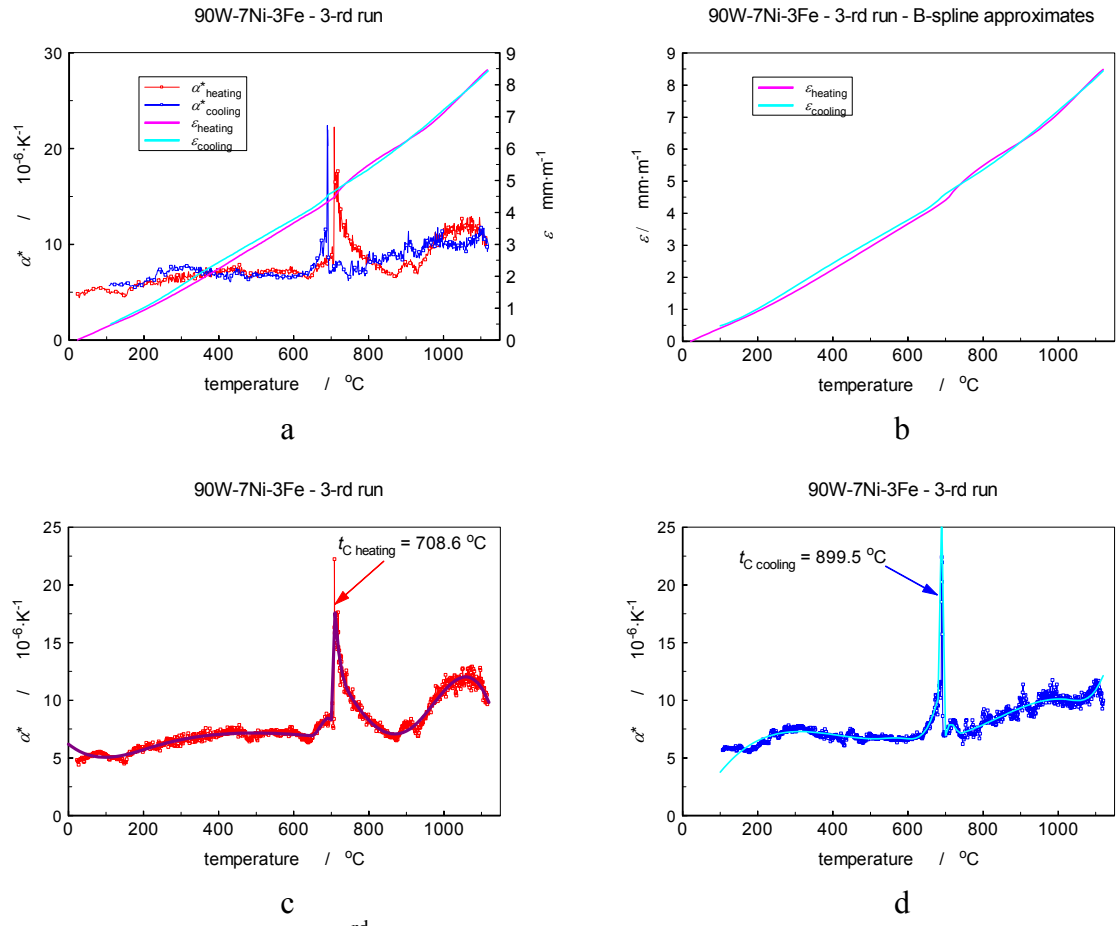

Figure 9. Results of 3rd run of dilatometric measurements (a) and effect of the LE experimental data approximation (b) together with results of CLTE* characteristics identification for heating (c) and cooling (d) from the approximated LE data

Analyzing the results one can notice inconsistency for about 0.7 % at 1120 °C in LE data. This discrepancy reflects initial inconsistency in experimental data and can not be attributed to the approximation procedure. The input data was not corrected for the temperature gradients[1]. However, it should be underlined that like in every approximation problem performance of fitting procedures at both ends of the data range usually is the weakest. Results shown in Figs 9 c and d confirm this observation. As was expected (comp. e.g. [4], [6], [11]) the fixed knot procedures were proved to be more reliable in data representation at the basic interval ends but they need additional information at the input.

5. Summary

The high thermal resolution dilatometric data from 90W-7Ni-3Fe tungsten heavy alloy investigation were numerically processed applying B-spline approximation procedures. The numerical analysis helped in inspection of the raw experimental data and enabled to establish representative thermal characteristics of the investigated property. The results were differentiated between heating and cooling. For the first time (comp. [2], [6] and [11]) the procedure of the spline approximation was applied for combined data from different experiments. There are

[1] The problem of the nonuniform temperature distribution within the interferometer system is discussed in [7].

promising outcomes from the performed analysis. The used procedures were proved to be not only well conditioned and effective in reconstruction of differential characteristics, helpful in detection of thermal characteristic singularities but also useful in providing the results averaged between different experimental runs.

The investigations, including numerical analyses results, provided data for further studies. The LE data will be applied in numerical modeling of heat transfer phenomena that occur during material sintering. The results of the phase transition investigation contribute to better understanding of the material under thermal cycling.

Acknowledgement

The research was supported by the State Committee of Scientific Research of Poland grant R 00 024 02 (2006-2010) and MUT project GW-HB 647 (2008).

References

[1] Grimvall, G.: *Thermophysical Properties of Materials*, Elsevier Sc. Publ. B. V., Amsterdam, 1986.

[2] Panas, A. J. and J. Terpiłowski: in *Proc. of the 7th International Symposium on Temperature and Thermal Measurements in Industry and Science TEMPMEKO'99*, May 30 – June 3, Delft 1999, pp. 493-498

[3] Björck, Å. and G. Dahlquist: *Numerical Methods*, Prentice-Hall, London, 1974.

[4] De Boor, C. 1976: *A Practical Guide to Splines*, Appl. Math. Sciences v. 27, Springer Verlag, Berlin, 1976.

[5] Ciesielski, Z.: *Theory of Spline Functions*, University of Gdańsk, Gdańsk, 1976/1977 (in Polish).

[6] Panas A. J.: *Achives of Thermodynamics*, 24 (4), 2003, pp. 47-65.

[7] Panas, A. J.: *The high thermal resolution investigation of the linear expansivity – Dilatometric thermal analysis*, Military University of Technology Monograph, Warsaw 1998, (in Polish).

[8] Panas A. J., Terpiłowsk J., Majewski T.: *Investigation of Thermophysical Properties of 53Ni-23Fe-24W Matrix Phase Component of WHA*, paper presented at the 18th European Conference on Thermophysical Properties, Pau, France, 31st August – 4th September 2008.

[9] Lassner, E., Schubert, D.W.: *Tungsten. Properties, Chemistry, Technology of the Element, Alloys and Chemical Compaunds* KluwerAcademic / Plenum Publishers, New York 1998, p.274.

[10] Taylor, R. E.: *Thermal Expansion of Solids*, CINDAS Data Series on Material Properties, V I-4, C. Y. Ho Editor, ASM International, Materials Park OH, 1998.

[11] Panas, A. J.: *Dilatometric Investigations of Phase Transitions Using B-Spline Data Processing*, in *Thermal Conductivity 27 / Thermal Expansion 15,* Wang H., Porter W. Eds., DEStech Publications, Inc., Lancaster PA, 2005, pp. 584-594.